Measuring Large Optical Transmission Matrices of Disordered Media

Hyeonseung Yu,[1] Timothy R. Hillman,[2] Wonshik Choi,[3] Ji Oon Lee,[4] Michael S. Feld,[2,*]
Ramachandra R. Dasari,[2] and YongKeun Park[1,†]

[1]*Department of Physics, Korea Advanced Institute of Science and Technology, Daejeon 305-701, South Korea*
[2]*G. R. Harrison Spectroscopy Laboratory, Massachusetts Institute of Technology, Cambridge, Massachusetts 02139, USA*
[3]*Department of Physics, Korea University, Seoul 136-701, South Korea*
[4]*Department of Mathematical Science, Korea Advanced Institute of Science and Technology, Daejeon 305-701, South Korea*

We report a measurement of the large optical transmission matrix (TM) of a complex turbid medium. The TM is acquired using polarization-sensitive, full-field interferometric microscopy equipped with a rotating galvanometer mirror. It is represented with respect to input and output bases of optical modes, which correspond to plane wave components of the respective illumination and transmitted waves. The modes are sampled so finely in angular spectrum space that their number exceeds the total number of resolvable modes for the illuminated area of the sample. As such, we investigate the singular value spectrum of the TM in order to detect evidence of open transmission channels, predicted by random-matrix theory. Our results comport with theoretical expectations, given the experimental limitations of the system. We consider the impact of these limitations on the usefulness of transmission matrices in optical measurements.

Optical wave propagation through highly scattering media is a fundamental physical phenomenon relevant to numerous fields including imaging through turbid media [1,2] and quantum information processing [3]. The scattering matrix is the linear transformation relating two monochromatic, propagating complex wave fields: that incident upon the sample; and that elastically scattered from it. The samples we consider are broad in lateral extent and are bounded (in the axial direction) by parallel-plane interfaces. Thus, all of the light may be regarded as entering and exiting the sample through the interfaces. The transmission matrix (TM) is a submatrix of scattering matrix, which describes propagation through the sample in a particular direction—light enters the sample at the ''front'' interface and exits (is scattered from) the ''back'' interface. The TM is generally expressed with respect to bases of the normal modes of the respective incident and scattered wave fields [4]. Each mode E_i is the complex-amplitude representation of the optical field corresponding to one particular polarization and propagation direction. The TM is therefore defined as the matrix t, with complex-valued entries t_{ij} connecting the incident optical field at the ith output mode to the jth input mode,

$$E_i^{\text{out}} = \sum_{j=1}^{N} t_{ij} E_j^{\text{in}}. \tag{1}$$

Common optical elements such as lenses or polarizers have simple TMs with low information content, as suggested by the fact that their effects on an incident wave field can be described using a simple equation. By contrast, disordered complex media such as paint layers or biological tissues have TMs with high information content; the enormous number of elements are apparently independent [5]. However, subtle correlations between the TM elements exist that can be discerned using statistical analysis. These correlations can give important insights into the mesoscopic properties of a complex medium. Additionally, knowledge of the TM can be used for imaging and focusing applications in environments with multiple light scattering [2,6–9].

The TM is a key concept in mesoscopic transport theory [4], and it has been directly measured in the microwave regime [10]. Previous, intensity-based experimental methods for considering light transport through complex media include: speckle pattern correlation [11], coherent backscattering [12,13], and vector transmission matrix measurement [14]. A significant breakthrough in optical-regime TM measurement has been achieved by using a phase-shifting interferometric system [15,16]. Although the number of measured TM matrix elements measured in these experiments was substantial (65 536 elements in the TM; 256 illumination and 256 detection modes in Ref. [15], for example), the full TM corresponding to the specified illuminated area of the sample is many times larger. Consequently, measurements of optical TMs reported so far do not seem to exhibit intrinsic correlations between the modes. This inference can be drawn from the fact that the distribution of singular values of the measured matrices obeys a quarter-circle law [15]. In fact, the number of resolvable modes, N, for either the incident or transmitted far-field illumination depends on the illuminated area of the sample, A, according to the equation $N = 2\pi A/\lambda^2$, where λ is the wavelength of the incident

light in the medium surrounding the sample. This equation accounts for the two orthogonal polarization states of the propagating wave field [17]. The modes can correspond to different plane wave angular (k vector) components of the respective beams (our choice, hereafter), or alternatively, different diffraction-limited spots at the respective interfaces.

In this Letter, we report a measurement of the large TM for a highly scattering medium. It was enabled by using a polarization-sensitive, full-field Mach-Zehnder interferometric microscope equipped with a fast two-axis rotating galvanometer mirror system. We measured the TM of an 18×18 μm^2 area of the medium, acquiring $21\,078 \times 21\,078$ entries, that is, a 420 million-element array. We investigate the singular-value and eigenvalue distribution of the TM in the context of random-matrix theory (RMT) developed by Dorokhov, Mello, Perreira, and Kumar (DMPK) [18,19]. Additionally, we consider the effect of the limited system numerical aperture (NA) in excluding the number of modes accessible to the system.

The experimental setup is shown in Fig. 1. A detailed description of the setup is discussed in Supplemental Material [20]. A plane wave beam from a linearly polarized He-Ne laser is first split into a sample and a reference arm. The two-axis rotating galvonometer mirror system controls the illumination angle of the beam impinging upon the scattering sample. The transmitted scattered beam is projected onto a camera, where the scattered beam interferes with a slightly tilted reference beam to generate off axis holograms for each illumination angle. Half-wave plates are located in both the sample and reference arms in order to control the axes of polarization of the beams.

The sample under study consists of a disordered layer of spray-painted ZnO nanoparticles with a thickness of $L = 10.5$ μm, sandwiched between two standard microscope cover slides. The layers were characterized through measurements of both their total and their angularly resolved transmission. From these measurements, we

determined the mean-free path to be $\ell = 0.63 \pm 0.14$ μm and the effective refractive index $n = 1.4 \pm 0.1$ at a free-space wavelength of 632.8 nm (See Supplemental Material [20]).

To construct the TM, we represent the measured scattered wave fields (at different illumination angles) as columns of k-vector coefficients. The k-space representation is generated by the two-dimensional Fourier transformation of the measured wave fields. The information is represented in a one-dimensional array whose entries are ordered according to increasing of the lateral wave vector modulus. This array comprises one half column in the TM matrix. The full column consists of the measured response for both output polarization states, corresponding to the input mode (Fig. 2).

We make two observations about the values presented in the matrix. Firstly, the moduli of the Fourier components of the measured wave fields decrease with increasing modulus $|k_{x,y}|$ of the lateral spatial frequency. This is primarily due to system vignetting and scattering through the side edges of the sample which cannot be measured by the CCD camera. These factors will have a distorting effect on the measured singular value spectrum, in addition to that of the limited measurement NA, as we describe below. Secondly, the horizontal lines that are particularly visible in the phase maps are measurement artifacts. These are due to unwanted diffraction by dust particles in the optical path. They can be removed in postprocessing, by subtracting the complex mean value of the matrix from each horizontal line. However, we have found this has no discernable effect on the measured eigenvalue distribution. As noted above, we matched the independent number of the input modes and the output modes at 21 078. The sampled number exceeds the resolvable number of input far-field modes ($2\pi A/\lambda^2 \approx 11\,000$) by a factor of about 2 for the measured field of view of 18×18 μm^2. The eigenvalues retrieved from the measured TM were appropriately rescaled by being divided by the oversampling ratio.
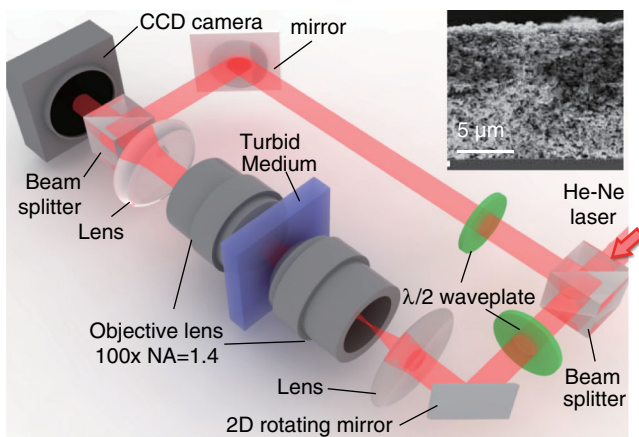

FIG. 1 (color online). Experimental setup. (Inset) scanning electron micrograph of a ZnO sample (cross section).
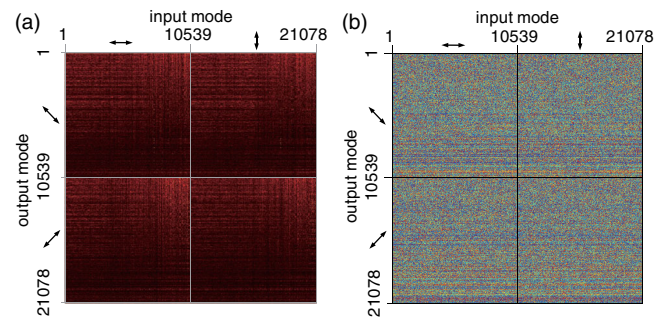

FIG. 2 (color online). (a) Amplitude and (b) phase of the reconstructed TM (a sampled representation of the rows and columns is shown). Row and column numbers indicate the spatial frequency mode indices of the outgoing and incoming complex wave fields, respectively. Arrows represent polarization direction.

We investigated the statistical properties of the measured large TM using RMT. We consider the transmission eigenvalues T_i of $tt^\dagger$, which are equal to the squared values of the singular values of the TM, λ_i. According to DMPK theory, for a highly scattering, but weakly absorbing medium, the probability density function of T_i is given by the equation [18,21],

$$p(T_i) = \langle T_i \rangle / (T_i \sqrt{1 - T_i}), \qquad \varepsilon < T_i < 1. \quad (2)$$

The parameter $\langle T_i \rangle \approx \ell/L$, is the mean transmittance of the distribution, and the value $\varepsilon = \cosh^{-2}(1/\langle T_i \rangle)$ is chosen so that $\int p(T)dT = 1$ [22]. This distribution has the important characteristic of being bimodal. A majority of the transmission channels (corresponding to input eigenvectors) will be either "open" or "closed", corresponding to almost-no transmission ($T_i \approx 0$) and near-complete transmission ($T_i \approx 1$), respectively [23,24].

The eigenvalue distributions calculated from the measured TM are shown in Fig. 3. The average transmission $\langle T_i \rangle$ was 0.0671. A simulated TM based on RMT [25] is also shown for the purpose of comparison. The normalized singular value distributions are shown in Fig. 3 (inset). For the comparison with the dimensionless theoretical predictions of RMT, the singular values λ_i are normalized to yield $\tilde{\lambda}_i = \lambda_i/\sqrt{\sum_{j=1}^{N} \lambda_j^2 / N}$. The distribution from the simulated TM clearly exhibits the expected bimodal distribution. The measured and simulated eigenvalue distributions are reasonably matched for low values ($T_i < 0.3$). However, beyond this threshold, the curves deviate strongly from one another. In particular, the open channels

are not observed in the measurement. One reason for this deviation may be the limited measurement NA, which leads to both imperfect control of the incident field and loss of some transmitted field information.

To test the effect of NA on the eigenvalue distribution, we numerically incorporate the limited-NA property into the RMT simulation. We achieve this by limiting the number of illumination and detection modes to a fraction f of the total number ($0 < f \leq 1$) for both the illumination and detection sides; we assume symmetry on the two sides. Then for the "reduced" transmission matrix, t_R entries corresponding to either $i, j > Nf$ are replaced with zeros. As shown in Fig. 3, the open channels are only observed in the ideal TM; with just 10% loss of optical modes, the open channels completely disappear. Also noteworthy is the fact that when $f = 0.65$, which is the experimental condition, the maximum values of the eigenvalue of the simulated TM ($T = 0.68$, $\lambda_i = 0.82$) is approximately equal to the maximum eigenvalue (0.65) obtained from the measurement.

There is a one-to-one correspondence between f and NA through the relationship $f = (NA)^2/n^2$. To see this, consider plane wave illumination with intensity I, polar angle θ with respect to the optical axis, upon a finite area A in a plane orthogonal to the optical axis. The total power intercepted by the area is equal to $IA \cos\theta$. We assume that the light scattering distribution is uniform in all directions, and that all entries of the TM have identical (marginal) probability distributions. Then, the canonical basis vectors of illumination and detection states (each corresponding to a small solid angle, $\Delta\Omega$, of illumination or detection, respectively) must have the property that $\cos\theta\Delta\Omega$ is constant. A solid angle element $\Delta\Omega$ represents surface area Δs of the unit sphere. The condition "$\cos\theta\Delta\Omega$ is constant" is equivalent to the condition that the area of the projection of Δs onto the equatorial plane be constant; thus, the
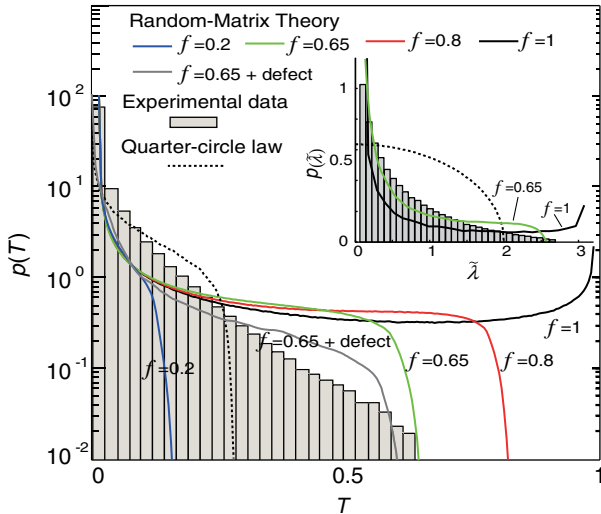

FIG. 3 (color online). Transmission eigenvalue distribution of the measured TM. The lines represent RMT simulations with full information (black line), information on only a fraction $f = 0.65$ of the incident and transmitted modes (green line), and incorporation of an additional defect factor of 24% (gray line). Dashed line represents distribution from the quarter-circle law. (Inset) Normalized singular values distribution of the measured TM.
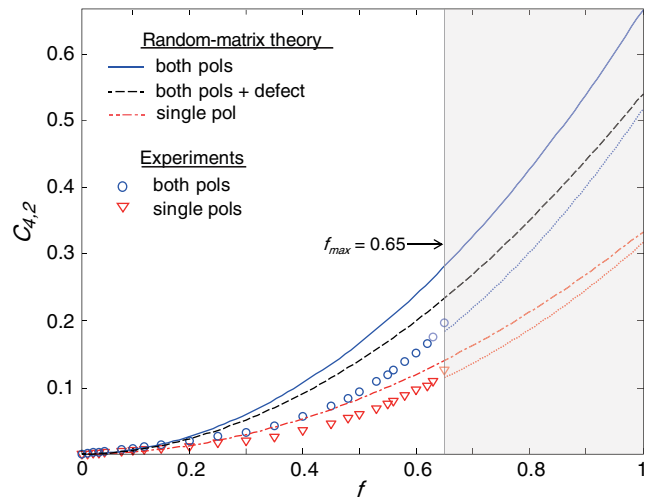

FIG. 4 (color online). Measured and ideal values for $C_{4,2}$ as a function of f. Dotted lines represent extrapolations from the measurements.

canonical basis states should be uniformly distributed over the two-dimensional lateral spatial frequency components of the wave field incident upon the scattering sample. The fraction of the total circular projection area corresponding to polar angles less than a given θ is equal to $\sin^2\theta = NA^2/n^2$.

In our experiment, from the effective NA of the objectives and the index of the immersion oil, we estimate $f = 0.65$. However, the distribution of the simulated eigenvalues with $f = 0.65$ deviates from the measured one, particularly at the high-eigenvalue end of the distribution. This deviation suggests an additional loss of information due to an uncollected component of the scattered field. The possible reasons for this loss could be (1) unwanted scattering by optical components or objects such as bubbles in the immersion oil, and (2) the aforementioned vignetting effects and the scattering of the beam to the side of the turbid sample, resulting in illumination that is not collected by the objective lens. We have attempted to incorporate this undesired information loss into our numerical simulation, by accounting for the lateral spread of the beam due to optical diffusion. We assume that 24% of the optical output modes were lost in the experiment. This value was calculated as follows. All incident modes cover the sample area of 18×18 μm^2. However, the average illumination profile on the output side will be expanded by a factor of approximately 1.31 (in area), the quantity being determined via convolution of the original spot profile with $\mathrm{sech}(x\sqrt{6}/l)$ [26]. Thus, $\sim 24\%$ (0.31/1.31) of the light and corresponding optical modes are lost in the experiments. To simulate this "defect", 24% of the output modes (randomly chosen) are replaced with zeros (gray line in Fig. 3), in a similar manner to the construction of the reduced transmission matrices, described above. The resulting RMT simulation shows improved agreement with the measured eigenvalue distribution.

The singular values λ_i of a large random matrix with independent, identically distributed entries will follow a quarter-circle distribution [27]. If correlations between the entries exist in our measured TM, we expect a deviation from this quarter-circle limit. The distribution for T_i corresponding to a quarter-circle law for λ_i is plotted in Fig. 3, clearly showing a different form to that of our experiment. By contrast, Popoff and co-workers [15] measured a relatively small fraction of the TM (we estimate $f < 0.001$ for their situation) and found a singular value distribution that nicely followed the quarter-circle law, indicating all correlations were lost from the matrix.

An important characteristic of the distribution $p(T_i)$ is $C_{4,2}$, the ratio of its second and first moments. Theoretically, $C_{4,2} = C_4/C_2 = \int T^2 p(T_i)dT / \int T p(T_i)dT = 2/3$. This value of $C_{4,2}$ is universal, i.e., independent of $\langle T_i \rangle$ or sample thickness. Recently, it has been demonstrated that TM can be used for focusing light [28] and image delivering [1,2]. From a theoretical point of view, the fraction $C_{4,2}$

gives the proportion of the incident power that is transmitted (on average) when wave front control of the incident beam is used to optimize the intensity at a point behind the turbid medium, regardless of the thickness of the sample [28]. One advantage of $C_{4,2}$ is that it can be directly estimated from the Hermitian matrix $H = (h_{i,j}) \equiv tt^\dagger$, without requiring that the eigenvalues be individually calculated. In the Supplemental Material [20], we show that the expected value of $C_{4,2}$ corresponding to a reduced TM is directly proportional to $NA_D^2 NA_I^2/n^4$, where NA_D^2 and NA_I^2 represent NA for the detection and illumination side, respectively. See Supplemental Material [20] for the derivation.

To investigate experimentally the effect of limited NA on $C_{4,2}$, we calculated its estimate $\hat{C}_{4,2}$ from the measured TM (Fig. 4). For the maximum value of f, the calculated $\hat{C}_{4,2}$ values are 0.180 (full polarization-dependent TM) and 0.117 (only one linearly polarization dependent for both input and output modes). These values are consistent with the report [28], where the maximum transmittance of an optimized beam was ~ 0.2 with a high-NA objective lens, a scattering sample with comparable optical properties, and the light polarization was considered.

To further address the effect of NA upon the values of $C_{4,2}$, we extrapolated the values of $\hat{C}_{4,2}$ for larger values of f than those permitted experimentally (dotted lines in Fig. 4). The extrapolation was obtained using the Matlab® fitting toolbox. The extrapolations for the cases of a single polarization and two polarizations showed trends similar to RMT predictions. The maximum values of the extrapolated $\hat{C}_{4,2}$ (for $f = 1$) was 0.32 (4% smaller than that expected from RMT) for the case of the unpolarized beam. When all polarization components were taken into account, the extrapolated $\hat{C}_{4,2}$ was 0.52, which is 22% smaller than expected from RMT. We attribute this deviation in the values of $C_{4,2}$ between the measurement and RMT mainly to the leakage of light to the side of the sample. When we simulate the values of $C_{4,2}$ considering 24% leakage in the TM, we obtained results that are comparable with those of the measurement.

In conclusion, we have demonstrated that large optical TM of a turbid medium can be experimentally measured using a fast two-axis galvanometer mirror and full-field interferometric microscopy equipped with a high-NA objective lens. Our work provides a means for directly measuring the TM and leads to observation of the intrinsic correlation between the modes of the measured optical TM. The total number of entries in the measured TM is approximately 420 million, which is slightly more than the number of resolvable modes for measured area of the 18×18 μm^2 field of view. Both the transmission eigenvalue and singular value distribution obtained from the measured TM deviate from the quarter-circle shape characteristic of a matrix with independent, random entries. This is in satisfactory agreement with the distribution

predicted theoretically, and simulated numerically, when corrected for the limited illumination and detection NAs. Our measurement method can be applied in situations where large transmission matrices are needed and will open new possibilities in focusing and imaging applications and will have many potential applications [1,2,7,29,30]. Furthermore, the present approach can be further expanded to the measurement of reflection matrices as well as scattering matrices. Moreover, localized optical modes [10,31] or modes of the evanescent near field resulting from multiple scattering of nanoparticles [32] may be accessed using measurement of the large TM.

Note added.—After submission of this Letter, a relevant theoretical paper appeared [33].

———

*Deceased.

†yk.park@kaist.ac.kr

[1] S. Popoff, G. Lerosey, M. Fink, A. C. Boccara, and S. Gigan, Nat. Commun. **1**, 81 (2010).

[2] Y. Choi, T. D. Yang, C. Fang-Yen, P. Kang, K. J. Lee, R. R. Dasari, M. S. Feld, and W. Choi, Phys. Rev. Lett. **107**, 023902 (2011).

[3] J. R. Ott, A. Mortensen, and P. Lodahl, Phys. Rev. Lett. **105**, 090501 (2010).

[4] C. W. J. Beenakker, Rev. Mod. Phys. **69**, 731 (1997).

[5] S. E. Skipetrov, Phys. Rev. E **67**, 036621 (2003).

[6] I. M. Vellekoop, A. Lagendijk, and A. P. Mosk, Nat. Photonics **4**, 320 (2010).

[7] A. P. Mosk, A. Lagendijk, G. Lerosey, and M. Fink, Nat. Photonics **6**, 283 (2012).

[8] J. H. Park, C. Park, H. Yu, Y.-H. Cho, and Y. Park, Opt. Express **20**, 17 010 (2012).

[9] J.-H. Park, C. Park, H. Yu, Y.-H. Cho, and Y. Park, Opt. Lett. **37**, 3261 (2012).

[10] Z. Shi and A. Z. Genack, Phys. Rev. Lett. **108**, 043901 (2012).

[11] J. H. Li and A. Z. Genack, Phys. Rev. E **49**, 4530 (1994).

[12] P. E. Wolf and G. Maret, Phys. Rev. Lett. **55**, 2696 (1985).

[13] M. P. Van Albada and A. Lagendijk, Phys. Rev. Lett. **55**, 2692 (1985).

[14] S. Tripathi, R. Paxman, T. Bifano, and K. C. Toussaint, Opt. Express **20**, 16067 (2012).

[15] S. M. Popoff, G. Lerosey, R. Carminati, M. Fink, A. C. Boccara, and S. Gigan, Phys. Rev. Lett. **104**, 100601 (2010).

[16] S. M. Popoff, G. Lerosey, M. Fink, A. C. Boccara, and S. Gigan, New J. Phys. **13**, 123021 (2011).

[17] D. Gabor, in *Progress in Optics*, edited by E. Wolf (North-Holland, Amsterdam, 1961), p. 109.

[18] O. N. Dorokhov, Solid State Commun. **51**, 381 (1984).

[19] P. Mello, P. Pereyra, and N. Kumar, Ann. Phys. (N.Y.) **181**, 290 (1988).

[20] See Supplemental Material at http://link.aps.org/supplemental/10.1103/PhysRevLett.111.153902 for the detailed experimental and analytical methods.

[21] J. Pendry, A. MacKinnon, and P. Roberts, Proc. R. Soc. A **437**, 67 (1992).

[22] M. C. W. van Rossum and T. M. Nieuwenhuizen, Rev. Mod. Phys. **71**, 313 (1999).

[23] J. B. Pendry, Physics **1**, 20 (2008).

[24] C. Beenakker, in *The Oxford Handbook of Random Matrix Theory*, edited by G. Akemann, J. Baik, and P. Francesco (Oxford University Press, Oxford, 2011), p. 723.

[25] D. Y. K. Ko, and J. C. Inkson, Phys. Rev. B **38**, 9945 (1988).

[26] I. M. Vellekoop, arXiv:0807.1087.

[27] V. Marčenko and L. A. Pastur, Math. USSR-SB **1**, 457 (1967).

[28] I. M. Vellekoop and A. P. Mosk, Phys. Rev. Lett. **101**, 120601 (2008).

[29] E. G. van Putten, D. Akbulut, J. Bertolotti, W. L. Vos, A. Lagendijk, and A. P. Mosk, Phys. Rev. Lett. **106**, 193905 (2011).

[30] M. Kim, Y. Choi, C. Yoon, W. Choi, J. Kim, Q.-H. Park, and W. Choi, Nat. Photonics **6**, 583 (2012).

[31] J. Wang and A. Z. Genack, Nature (London) **471**, 345 (2011).

[32] J.-H. Park, C. Park, H. Yu, J. Park, S. Han, J. Shin, S. H. Ko, K. T. Nam, Y.-H. Cho, and Y. Park, Nat. Photonics **7**, 454 (2013).

[33] A. Goetschy and A. D. Stone, Phys. Rev. Lett. **111**, 063901 (2013).